Transient Variability In Vapor Intrusion And The Factors That Influence It

Jonathan G. V. Ström,[†] Yijun Yao,[‡] and Eric M. Suuberg[*,†]

†*Brown University, School of Engineering, Providence, RI, USA*

‡*Zhejiang University, Hangzhou, China*

E-mail: eric_suuberg@brown.edu

Abstract

Introduction

Long term vapor intrusion (VI) studies in both residential and larger commercial structures have raised concerns regarding significant observed transient behavior in indoor air contaminant concentrations.[1–7] VI involves the migration of volatilizing contaminants from soil, groundwater or other subsurface sources into overlying structures. VI has been a recognized problem for some time, but many aspects remain poorly understood, particularly with respect to the causes of large temporal transients in indoor air concentrations. There is uncertainty within the VI community regarding how to best develop sampling strategies to address this problem.[1,3,8]

Results from a house operated by Arizona State University (ASU) near Hill AFB in Utah, an EPA experimental house in Indianapolis, IN and a large warehouse at the Naval Air Station (NAS) North Island, CA have all shown significant transient variations in indoor

air contaminant concentrations. All were outfitted with sampling and monitoring equipment that allowed tracking temporal variation in indoor air contaminant concentrations on time scales of hours. All have shown that these concentrations varied significantly with time - orders of magnitude on the timescale of a day or days.[5,9,10]

In one instance the source of the variation was clearly established during the study; at the ASU house a field drain pipe (or "land drain"), which connected to a sewer system, was discovered beneath the house, and careful isolation of this source led to a clear conclusion that this preferential pathway significantly contributed to observed indoor air contaminant levels and their fluctuations.[10,11] While in this case the issue of a contribution from a preferential pathway was clearly resolved, what it left open was a question of whether existence of such a preferential pathway to an area beneath a structure would always be expected to lead to large fluctuations in indoor air contaminant concentrations.

Similarly, a sewer pipe has recently been suggested to be a source of the contaminants found in the EPA Indianapolis house. That site was also characterized by large indoor air contaminant concentration fluctuations.[7,12] Sewer lines have been generally implicated as VI sources at several sites.[12–15] A Danish study estimate that roughly 20% of all VI sites in central Denmark involve significant sewer VI pathways.[16] Thus while the consideration of a role of possible sewer or other preferential pathways is now part of normal good practice in VI site investigation,[1] it is still not known whether the existence of such pathways automatically means that large temporal fluctuations are necessarily to be expected. In some of these cited cases,[13,15] a sewer provided a pathway for direct entry of contaminant into the living space. While potentially important in many cases, this scenario is not further considered here, where the focus is on pathways that deliver contaminant via the soil beneath a structure.

It is, however, now known that even absent a preferential pathway, there may be significant transient variation in indoor air contaminant concentrations at VI sites.[2,4,17] One example is a site at NAS North Island at which no preferential pathways have been identified. Instead, a building at this site is characterized by significant temporal variations in

indoor-outdoor pressure differential.[5] It is believed that this is the origin of the observed indoor air contaminant concentration fluctuations at that site.

This paper investigates the sources of the temporal variation in indoor air contaminant concentrations in both the presence and absence of preferential pathways. In this work, the latter scenarios are referred to as "normal" VI scenarios, in which there is typically a groundwater source of the contaminant. Specifically, we pose the question of just how much variation in indoor air contaminant concentration may be expected at such normal VI sites vs. those characterized by preferential pathways. The conditions required for preferential pathways to become significant contributors to temporal variations in indoor air contaminant concentrations are also explored, and the consequences for sampling strategies are also discussed.

Methods

Statistical Analysis Of Field Data

To begin to characterize transient behavior in indoor air contaminant concentrations, actual datasets are analyzed to establish common levels of variability at VI sites. For this purpose, the datasets from the ASU house in Utah, the EPA Indianapolis site and North Island NAS were chosen for analysis. This paper relies on statistical analysis of published field data, and readers are referred to the original works for details regarding data acquisition.[3,5,7,9,10]

The ASU house data were obtained over a period of a few years. During part of this time, controlled pressure method (CPM) tests were being conducted, in which the house was underpressurized to an extent greater than that characterizing "normal" operation. This caused greater than normal advective flow from the subsurface into the house, thus increasing VI potential.[6,9,18] This period of CPM testing is considered separately from the otherwise "natural" VI conditions in the analysis. Likewise, the existence of a preferential pathway at the ASU house needs to be considered in examining the dataset, noting that

during some of the testing, this pathway was deliberately cut off, resulting in what we have termed "normal" VI conditions in which the main source of contaminant was believed to be groundwater.

The NAS North Island dataset has not (as far as is known) been influenced by a preferential pathway, but the structure there was subject to large internal pressure fluctuations, much more extensive than those typically recorded at the ASU house during normal operations. Additionally, the underlying soil at NAS North Island is sandy and more permeable than that at the ASU site, which, as will be shown, contributes to the indoor air contaminant concentrations being more sensitive to pressure fluctuations.[5]

Likewise, the Indianapolis site investigation spanned a number of years and periodically included the testing of a sub-slab depressurziation system (SSD). The goal of the SSD testing was to mitigate the VI risk by drastically depressurizing the sub-slab area underneath the house, preventing the contaminants from entering the structure above. Only the period before the installation of this system was considered in the present analysis. It is likely a sewer line beneath the structure acted as a preferential pathway,[12] however at no point was this preferential pathway removed, making it difficult to assess how significant the role of the preferential pathway was at this site. Regardless of this it is of interest to consider the data from this site due to how extensive and complete the data collection was.

The typical variation in indoor air contaminant concentrations with time will first be considered below in the case of the ASU house during "natural", (i.e. non-CPM conditions), in the case of the NAS North Island site over the entire available dataset, and for the Indianapolis case we consider the variations before the installation of the SSD system. The deviations in indoor air concentration from the mean TCE (and Chloroform and PCE at the Indianapolis site) values, as well as the indoor-outdoor pressure differentials associated with these concentrations were examined. Both univariate and bivariate kernel density estimations (KDE) were constructed. KDE is a technique that estimates the probability distribution of a random variable(s) by using multiple kernels, or weighting functions, and

in this case, Gaussian kernels are used to create the KDEs. This means that it is presumed that the variables of interest (i.e., indoor air contaminant concentrations and indoor-outdoor pressure differentials, as sampled) are normally distributed around mean values (and that there are statistical fluctuations associated with each sampling event). In this instance, the scipy statistical package was used to construct the KDEs, assuming a bandwidth parameter determined by Scott's rule. The distributions of the individual parameters and the relationship between them will be examined using the KDE method.

Modeling Work

In addition to examining the actual field data, a previously described three -dimensional computational fluid dynamics model of a generic VI impacted house was used to elucidate certain aspects of the processes. This model was implemented in a finite element solver package, COMSOL Multiphysics. In the present work, there has been an addition of a preferential pathway to the "standard" model that has been described before in publications by this group.[19–21] As in the earlier studies, only the vadose zone soil domain is directly modeled.

The modeled structure is assumed to have a 10x10 m foundation footprint, with the bottom of the foundation slab lying 1 m below ground surface (bgs), simulating a house with a basement. The indoor air space is modeled as a continuously stirred tank (CST)[1] and all of the contaminant entering the house is assumed to enter with soil gas through a 1 cm wide crack located between the foundation walls and the foundation slab around the perimeter of the house. All of the contaminant leaving the indoor air space is assumed to do so via air exchange with the ambient. The indoor control volume is assumed to consist of only of the basement, assumed as having a total volume of 300 m^3. Clearly different assumptions could be made regarding the structural features and the size of the crack entry route, but for present purposes, this is unimportant as the intent is only to show for "typical" values what the influence of certain other features can be.

The modeled surrounding soil domain extends 5 meters from the perimeter of the house, and is assumed to consist of sandy clay (except as noted). Directly beneath the foundation slab, there is assumed to be a 30 cm (one foot) thick gravel layer, except in certain cases where this sub-base material is assumed to be the same as the surrounding soil (termed a "uniform" soil scenario).

Where relevant The preferential pathway is modeled as a 10 cm (4") pipe that exits into the gravel sub-base beneath the structure. The air in the pipe is assumed to be contaminated with TCE at a vapor concentration equal to the vapor in equilibrium with the groundwater contaminant concentration below the structure, modified by a scaling factor χ, allowing the contaminant concentration in the pipe to be parameterized.

The groundwater beneath the structure is assumed to be homogeneously contaminated with trichloroethylene (TCE) as a prototypical contaminant. The groundwater itself is not modeled, as the bottom of the model domain is defined by the top of the water table. The ground surface and the pipe are both assumed to be sources of air to the soil domain. Both are assumed to be at reference atmospheric pressure.

Vapor transport in the soil is governed by Richard's equation, a modified version of Darcy's Law, taking the variability of soil moisture in the vadose zone into account.[22] The van Genuchten equations are used to predict the soil moisture content and thus the effective permeability of the soil.[23] The effective diffusivity of contaminant in soil is calculated using the Millington-Quirk model.[24] The transport of vapor contaminant in the soil is assumed to be governed by the advection-diffusion equation, in which either advection or diffusion may dominate depending upon position and particular circumstances. The equations and the boundary conditions are given in Table 1.

Table 1: Governing equations, boundary conditions & model input parameters. (See below for table of nomenclature).

(a) Governing equations

Unsteady-CSTR	$V\frac{du}{dt} = \int_{A_{\text{ck}}} j_{\text{ck}} dA - uA_eV$
Richard's equation	$\nabla \cdot \rho\Big(-\frac{\kappa_s}{\mu} k_r \nabla p\Big) = 0$
Millington-Quirk	$D_{\text{eff}} = D_{\text{air}}\frac{\theta_g^{10/3}}{\theta_t^2} + \frac{D_{\text{water}}}{K_H}\frac{\theta_w^{10/3}}{\theta_t^2}$
Advection-diffusion equation	$\frac{\partial}{\partial t}\Big(\theta_w c_w + \theta_g c\Big) = \nabla(D_{\text{eff}} \cdot \nabla c) - \vec{u} \cdot \nabla c$
van Genuchten equations	$\text{Se} = \frac{\theta_w - \theta_r}{\theta_t - \theta_r} = [1 + \lvert\alpha z\rvert^n]^{-m}$ $\theta_g = \theta_t - \theta_w$ $k_r = (1 - \text{Se})^l[1 - (\text{Se}^{-m})^m]^2$ $m = 1 - 1/n$

(b) Boundary conditions

Boundary	**Richard's equation**	**Advection-diffusion equation**
At foundation crack	$p = p_{\text{in/out}}$ (Pa)	$j_{\text{ck}} = \frac{uc}{1-\exp(uL_{\text{slab}}/D_{\text{air}})}$
At groundwater source	N/A	$c = c_{\text{gw}}K_H$ (μg/m^3)
At ground surface	$p = 0$ (Pa)	$c = 0$ (μg/m^3)
Exit of preferential pathway	$p = 0$ (Pa)	$c = c_{\text{gw}}K_H\chi$ (μg/m^3)

(c) Soil & gravel properties[25–27]

Soil	Permeability (m^2)	Density (kg/m^3)	θ_s	θ_r	α (1/m)	n
Gravel	$1.3 \cdot 10^{-9}$	1680	0.42	0.005	100	3.1
Sand	$9.9 \cdot 10^{-12}$	1430	0.38	0.053	3.5	3.2
Sandy Clay	$1.7 \cdot 10^{-14}$	1470	0.39	0.12	3.3	1.2

(d) Trichloroethylene (diluted in air) properties[26,27]

D_{air} (m^2/h)	D_{water} (m^2/h)	Density (kg/m^3)	Viscosity (Pa $\cdot$ s)	K_H	M (g/mol)
$2.47 \cdot 10^{-2}$	$3.67 \cdot 10^{-6}$	1.614	$1.86 \cdot 10^{-5}$	0.403	131.39

(e) Building properties

V_{base} (m^3)	L_{slab} (cm)	A_e (1/hr)
300	15	0.5

Results & Discussion

Statistical Analysis of Field Data

Our discussion of examining the temporal variability of indoor air contaminant concentration begins by considering one of the most dynamic factors that influence VI - the indoor/outdoor

Figure 1: Distributions of indoor/outdoor pressure differences (top row), and its correlation with indoor air contaminant concentrations (middle rows), and air exchange rate (bottom row), at three different VI sites - ASU house, Indianapolis site, and North Island NAS.

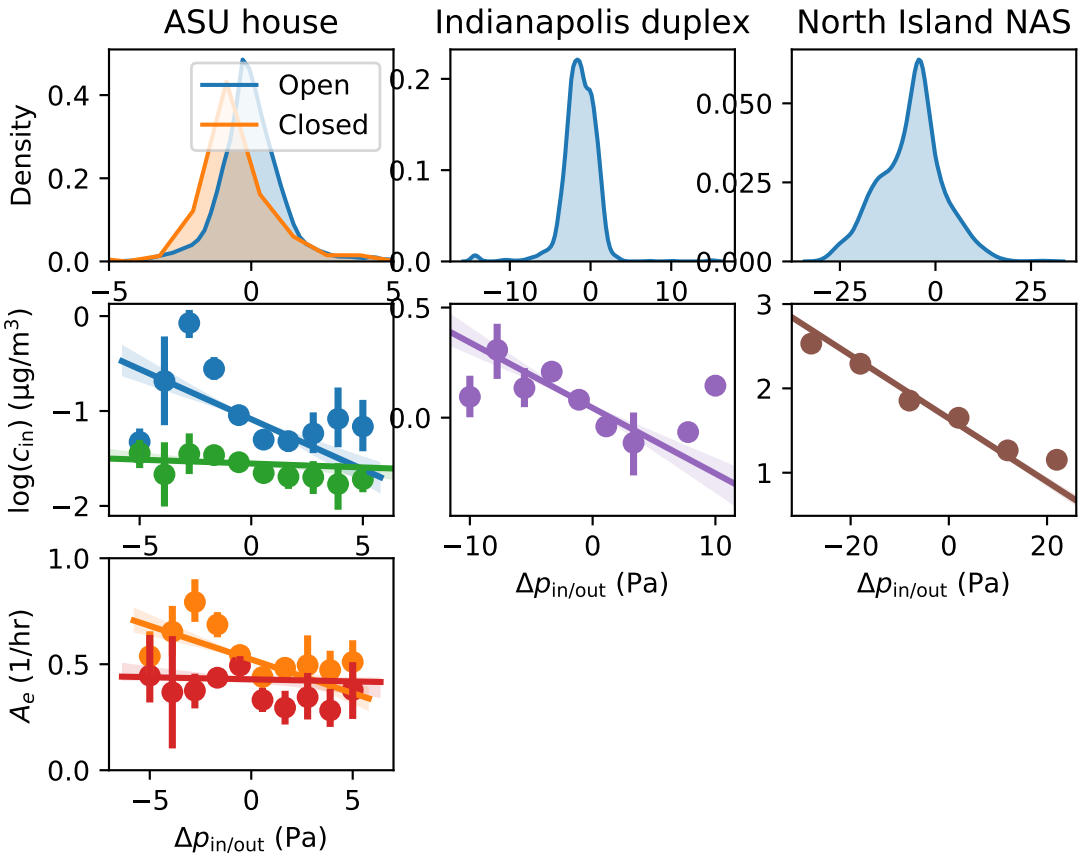

pressure difference ($p_{\text{in/out}}$). In the top row of Figure 1, the distribution of $p_{\text{in/out}}$ at three difference VI sites, the ASU house, Indianapolis site, and North Island NAS, are plotted. The distributions of $p_{\text{in/out}}$ at these three site resemble normal-like distribution, with a mean of a few negativa Pa, indicating that the most probable state is that these sites are slightly depressized. At the ASU house and the Indianapolis site, the range of $p_{\text{in/out}}$ values are relatively similar, whereas the North Island NAS site has significalty larger span of values. This is most likely due to the poor structural condition of the North Island site, making it much more suspectible to barometric pressure fluctations; the ASU house and Indianapolis site are regular residential structure in good condition. The periods when the preferential

pathway at the ASU house was open and closed are considered separately.

Now we move on to look at $p_{\text{in/out}}$ is correlated with the indoor air contaminant concentration (c_{in}). The middle row of Figure 1 shows the log-10 values of c_{in} vs. $p_{\text{in/out}}$, placed into evenly spaced bins, are plotted. Each bin represents the mean c_{in} and the errorbars show the 95% confidence interval. A linear regression curve is also fitted to the data, with the shaded part of the regression again indicating the 95% confidence interval. At the ASU house, it is readibly apparent that the preferential pathway has a profound effect on how sensitive c_{in} is to $p_{\text{in/out}}$, showing that the closing of the preferential pathway fundamentally changes the site. Perhaps surprsingly, when the preferential pathway is closed $p_{\text{in/out}}$ is not strongly correlated with c_{in}.

At the Indianapolis and North Island NAS sites, we again see the association of higher c_{in} when the structures are depressurized, but with still significant variability for a given $p_{\text{in/out}}$.

The difference in correlation of c_{in} vs. $p_{\text{in/out}}$ for the "open" and "closed" periods, as well as the $p_{\text{in/out}}$ is more evenly distributed around 0 Pa support our choice of model, where we assume that the preferential pathway acts by enhancing the "advective potential" of a VI site through improving communication between the indoor and outdoor.

It is clear that $p_{\text{in/out}}$ sets a trend, i.e. increased depressurziation is associated with higher c_{in}, but there is still considerable variability for a given $p_{\text{in/out}}$. $p_{\text{in/out}}$ is important in determining the contaminant entry rate into a structure, but it also will partly determine the air exchange rate. How significantly $p_{\text{in/out}}$ determines A_e varies with site specific conditions, e.g. HVAC operation, if windows are open/closed, how well insulted the structure is etc. A_e is thus highly variate for a given $p_{\text{in/out}}$, and we hypothesize that most of the variability in c_{in} at a specific $p_{\text{in/out}}$ may be explained by variation in air exchange rate (A_e). In the bottom left of Figure 1 we can see that larger depressurziation is associated with higher A_e, while overpressurazation is associated with lower A_e, but with still significant uncertainty.

Influence Of Pressure On Indoor Air Variability

Figure 2: Simulated cases

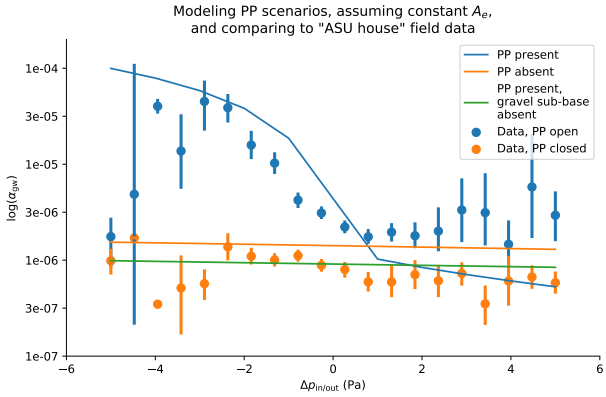

To examine the role that $p_{\text{in/out}}$ and A_e play in determining c_{in} variability (given as attenuation from groundwater vapor source α_{gw} here), we first consider modeling VI scenarios with a constant $A_e = 0.5$ (1/hr) (the mean A_e at the ASU house), and varying $p_{\text{in/out}}$ from 5 to -5 Pa. The first of these scenarios is aimed to be similar to the period when the preferential pathway is open at the ASU house, and thus the modeled preferential pathway is active. In the second scenario, this preferential pathway feature is deactivated, akin to the period when the preferential pathway was closed at the ASU site. And in the third, the preferential pathway is again modeled, but the permeable gravel sub-base is instead assumed consist of the sandy loam, just like the surrounding soil, giving an "uniform soil" scenario. The results of these modeled scearios are then compared to the preferential pathways "open" and "closed" periods from the ASU data, and may be seen in Figure 2. The data is here binned into evenly spaced bins, with each dot representing the mean α_{gw} and the error bars denote the 95% confidence intervals.

By examining the first scenario (blue) it is readily apparent that the model is able to capture the behavior of the preferential pathway when the structure is depressized ($p_{\text{in/out}} < 0$) but not very well when the house is overpressurized ($p_{\text{in/out}} > 0$). This shows that the preferential pathways acts by increasing advective potential, allowing even relatively

small increases in depressurziation dramatically increases the contaminant entry rate into the house. Conversely, when the structure is overpressurized, contaminant entry is more effectively inhibited, leading to diffusion being the more important transport mechanism from the sub-base to the indoor air space, leading to the decrease in α_{gw}. Yet, when $p_{\text{in/out}} > 0$ there is a slight increase in α_{gw} which can be explained by the fact that lower A_e are associated with overpressurazation, leading to an increase in α_{gw},

An interesting contrast to this scenario is third, when the preferential pathway is still present but the permeable gravel sub-base is not. Under these conditions, there is almost increase in advective transport as the impermeable sub-base effectively inhibits this. This leads to the conclusion that a unless there is some way for a preferential pathway to effectively communicate between the sub-base region (or wherever the preferential pathway is), then it is unlikely to find the dramatic effect observed at the ASU house.

Lastly, we consider the second scenario, where there is no preferential pathway present (but there is a permeable gravel sub-base). Here the general (weak) trend of increased α_{gw} with increase depressurziation is captured, but none of the variability is captured. There is inadequate potential for advective transport and thus $p_{\text{in/out}}$ does not significantly increase the contaminant entry rate. Furthermore, the seemingly random variability is not captured. Clearly, the A_e fluctations must be incorporated into the modeling methodoly to more accurately predict the variability in α_{gw}.

Combined Influence Of Pressure And Air Exchange Rate On Indoor Air Variability

To predict the variability of α_{gw} for a given pressure, we use the minimum and maximum A_e values observed at the ASU site (0.06 and 3.38 per hour respectively), and calculate α_{gw} over the same range of $p_{\text{in/out}}$ values. This gives the range of values that α_{gw} may fluctuate over for a given $p_{\text{in/out}}$. Using this method, the analysis in Figure 2 is repeated, i.e. that the cases when the preferential pathways is open and closed respectively are considered. The

Figure 3: Simulated cases

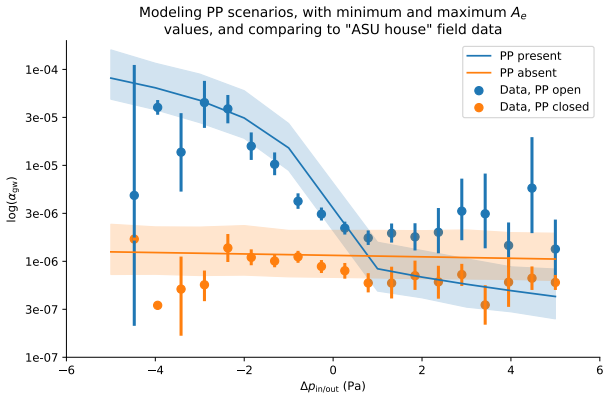

result of this analysis can be seen in Figure 3, where this range of α_{gw} is represented by the shaded areas, and the solid line is the predicted α_{gw} when A_e assumes the mean value of 0.50 per hour.

Variation Timeperiod

Figure 4: (1D is 1 day, 2W is 2 weeks, and 3M is 3 months).

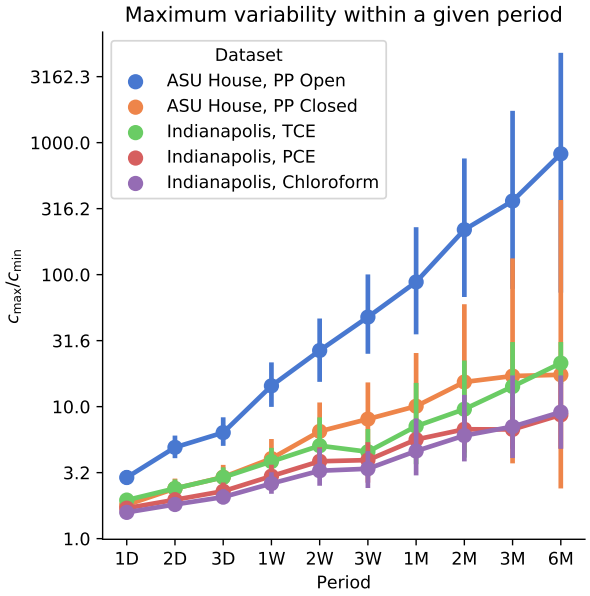

So far our discussion has focused on how much variability in c_{in} can be expected, and some drivers for this, at the three different sites. However, this tells just little about how much

c_{in} may vary over a given timeperiod. To examine this, the data is resampled over a chosen timeperiod, and the quotient of the maximum and minimum c_{in} (denoted as c_{max}/c_{min}) are plotted for this period. I.e. if c_{in} samples were collected every four hours over a period of a year, and the data is resampled on a daily basis, then c_{max}/c_{min} is returned for within each day, giving 365 data points. For this analysis, we consider the period when the preferential pathway was open/closed at the ASU house, and the three indoor air contaminant found at the Indianapolis site (TCE, PCE, and Chloroform). The North Island NAS dataset is excluded here, as the data that we have available only spans a few days versus year(s) for the ASU house and Indianapolis sites.

Figure 4 shows the the expected maximum variability over different resampling periods (from 1 day to 6 months). As one might expect, the longer the resampling period, the larger the maximum variability is, spanning from less than a threefold difference, to two to three orders of magnitude. That such a large variability is observed when the resampling time approaches the length of the entire datasets is hardly surprising, nor is it surprising that the variability is much more significant when the preferential pathway was open than closed. What may be surprising is that absent a preferential pathway such as the one at the ASU house, it may may take a few weeks before an order of magnitude maximum variability is reached. The most significant result of this analysis is that the maximum variability is quite small across a few days, suggesting that e.g. 24-hour passive samplers will resolve the daily temporal variabilty in c_{in} well ($c_{max}/c_{min} \approx 1.5$) and that a sampling frequency greater than a few days may yield little extra information.

Attenuation To Subslab

Acknowledgement

This project was supported by grant ES-201502 from the Strategic Environmental Research and Development Program and Environmental Security Technology Certification Program

(SERDP-ESTCP).

References

(1) U.S. Environmental Protection Agency, OSWER Technical Guide for Assessing and Mitigating the Vapor Intrusion Pathway From Subsurface Vapor Sources To Indoor Air. https://www.epa.gov/sites/production/files/2015-09/documents/oswer-vapor-intrusion-technical-guide-final.pdf, 00005.

(2) Folkes, D.; Wertz, W.; Kurtz, J.; Kuehster, T. Observed Spatial and Temporal Distributions of CVOCs at Colorado and New York Vapor Intrusion Sites. *29*, 70–80, 00048.

(3) Holton, C.; Luo, H.; Dahlen, P.; Gorder, K.; Dettenmaier, E.; Johnson, P. C. Temporal Variability of Indoor Air Concentrations under Natural Conditions in a House Overlying a Dilute Chlorinated Solvent Groundwater Plume. *47*, 13347–13354, 00028.

(4) Johnston, J. E.; Gibson, J. M. Spatiotemporal Variability of Tetrachloroethylene in Residential Indoor Air Due to Vapor Intrusion: A Longitudinal, Community-Based Study. *24*, 564, 00018.

(5) Hosangadi, V.; Shaver, B.; Hartman, B.; Pound, M.; Kram, M. L.; Frescura, C. High-Frequency Continuous Monitoring to Track Vapor Intrusion Resulting From Naturally Occurring Pressure Dynamics. *27*, 9–25, 00001.

(6) McHugh, T.; Loll, P.; Eklund, B. Recent Advances in Vapor Intrusion Site Investigations. *204*, 783–792, 00005.

(7) U.S. Environmental Protection Agency, Assessment of Mitigation Systems on Vapor Intrusion: Temporal Trends, Attenuation Factors, and Contaminant Migration Routes under Mitigated And Non-Mitigated Conditions. 00002.

(8) Johnson, P. C.; Holton, C. W.; Guo, Y.; Dahlen, P.; Luo, E. H.; Gorder, K.; Dettenmaier, E.; Hinchee, R. E. Integrated Field-Scale, Lab-Scale, and Modeling Studies for Improving Our Ability to Assess the Groundwater to Indoor Air Pathway at Chlorinated Solvent-Impacted Groundwater Sites. 00003.

(9) Holton, C. W. Evaluation of Vapor Intrusion Pathway Assessment Through Long-Term Monitoring Studies. `https://repository.asu.edu/attachments/150778/content/Holton_asu_0010E_15040.pdf`, 00003.

(10) Guo, Y. Vapor Intrusion at a Site with an Alternative Pathway and a Fluctuating Groundwater Table. `https://repository.asu.edu/items/36435`, 00001.

(11) Guo, Y.; Holton, C.; Luo, H.; Dahlen, P.; Gorder, K.; Dettenmaier, E.; Johnson, P. C. Identification of Alternative Vapor Intrusion Pathways Using Controlled Pressure Testing, Soil Gas Monitoring, and Screening Model Calculations. *49*, 13472–13482, 00019.

(12) McHugh, T.; Beckley, L.; Sullivan, T.; Lutes, C.; Truesdale, R.; Uppencamp, R.; Cosky, B.; Zimmerman, J.; Schumacher, B. Evidence of a Sewer Vapor Transport Pathway at the USEPA Vapor Intrusion Research Duplex. *598*, 772–779, 00007.

(13) Pennell, K. G.; Scammell, M. K.; McClean, M. D.; Ames, J.; Weldon, B.; Friguglietti, L.; Suuberg, E. M.; Shen, R.; Indeglia, P. A.; Heiger-Bernays, W. J. Sewer Gas: An Indoor Air Source of PCE to Consider During Vapor Intrusion Investigations. *33*, 119–126, 00022.

(14) Roghani, M.; Jacobs, O. P.; Miller, A.; Willett, E. J.; Jacobs, J. A.; Viteri, C. R.; Shirazi, E.; Pennell, K. G. Occurrence of Chlorinated Volatile Organic Compounds (VOCs) in a Sanitary Sewer System: Implications for Assessing Vapor Intrusion Alternative Pathways. *616-617*, 1149–1162, 00002.

(15) Riis, C. E.; Christensen, A. G.; Hansen, M. H.; Husum, H.; Terkelsen, M. Vapor Intrusion through Sewer Systems: Migration Pathways of Chlorinated Solvents from Ground-

water to Indoor Air. Seventh International Conference on Remediation of Chlorinated and Recalcitrant Compounds. 00012.

(16) Nielsen, K. B.; Hvidberg, B. Remediation Techniques for Mitigating Vapor Intrusion from Sewer Systems to Indoor Air. *27*, 67–73, 00002.

(17) Brenner, D. Results of a Long-Term Study of Vapor Intrusion at Four Large Buildings at the NASA Ames Research Center. *60*, 747–758, 00003.

(18) McHugh, T. E.; Beckley, L.; Bailey, D.; Gorder, K.; Dettenmaier, E.; Rivera-Duarte, I.; Brock, S.; MacGregor, I. C. Evaluation of Vapor Intrusion Using Controlled Building Pressure. *46*, 4792–4799, 00037.

(19) Shen, R.; Pennell, K. G.; Suuberg, E. M. Influence of Soil Moisture on Soil Gas Vapor Concentration for Vapor Intrusion. *30*, 628–637, 00015 WOS:000325689400005.

(20) Yao, Y.; Wang, Y.; Zhong, Z.; Tang, M.; Suuberg, E. M. Investigating the Role of Soil Texture in Vapor Intrusion from Groundwater Sources. *46*, 776–784, 00003.

(21) Yao, Y.; Mao, F.; Ma, S.; Yao, Y.; Suuberg, E. M.; Tang, X. Three-Dimensional Simulation of Land Drains as a Preferential Pathway for Vapor Intrusion into Buildings. *46*, 1424–1433, 00002.

(22) Richards, L. A. Capillary Conduction of Liquids through Porous Mediums. *1*, 318–333, 05183.

(23) van Genuchten, M. T. A Closed-Form Equation for Predicting the Hydraulic Conductivity of Unsaturated Soils. *44*, 892–898, 00004.

(24) Millington, R. J.; Quirk, J. P. Permeability of Porous Solids. *57*, 1200, 01808.

(25) Dan, H.-C.; Xin, P.; Li, L.; Li, L.; Lockington, D. Capillary Effect on Flow in the Drainage Layer of Highway Pavement. *39*, 654–666, 00007.

(26) Abreu, L. D. V.; Schuver, H. Conceptual Model Scenarios for the Vapor Intrusion Pathway. https://www.epa.gov/sites/production/files/2015-09/documents/vi-cms-v11final-2-24-2012.pdf, 00010.

(27) U.S. Environmental Protection Agency, Users's Guide For Evaluating Subsurface Vapor Intrusion Into Buildings. https://www.epa.gov/sites/production/files/2015-09/documents/2004_0222_3phase_users_guide.pdf, 00000.